Turbulent impulsive magnetic energy release from electron scale reconnection

W. Horton, J.-H. Kim, and F. Militello
Institute for Fusion Studies, The University of Texas at Austin, Austin, Texas 78712

M. Ottaviani
Association Euratom- CEA DRFC, CEA Cadarache 13108, Saint-Paul-Lez-Durance, France

(Received 3 August 2006; accepted 30 November 2006; published online 9 January 2007)

Magnetic reconnection may occur as bursts of nonlinear plasma dynamics on the electron collisionless skin length scale $d_e=c/\omega_{pe}$, during which a large fraction of the magnetic energy is converted to plasma thermal energy and plasma flow energy. An example of such a bursty energy release event is given with a simple set of electron Hall equations. The energization mechanism is the cross-field compression of the electron gas between interacting magnetic islands. The electron energization appears to be consistent with the rapid electron energy flux changes measured by the Cluster spacecraft crossing thin current sheets at $-17\ R_E$ in the geotail. The analysis is relevant to planned spacecraft missions for measuring electron scale magnetic reconnection events in the geomagnetic tail. © *2007 American Institute of Physics*. [DOI: 10.1063/1.2424555]

I. INTRODUCTION

Magnetic reconnection modelling has a long and complicated history.[1,2] In the domain of collisionless magnetic reconnection, there are two space-time scales of the dynamics. One is the ion tearing mode dynamics where the nonlinear structure and islands are large compared to ion gyroradius ρ_i and the ion inertial scale length $\rho_s=(m_iT_e)^{1/2}/eB$, and the second is the formation of small scale structures and islands on the scale of electron[3] skin depth $d_e=c/\omega_{pe}$ and up to the scale of the ion inertial scale $\rho_s \geqslant c/\omega_{pe}$. The time scale for the electron event is correspondingly shorter than that for the ion events, and they have a larger power transfer from the magnetic energy releases $\Delta E_B<0$.

The short duration and large numbers of such events make them an ideal candidate to explain the fast, sometimes called explosive, energy release required by geomagnetic substorms. The time scale for the collisionless ion tearing modes is generally too long for the fast dynamics $\Delta t \ll 100L/v_A<10$ min observed in geomagnetic substorms.

For geotail reconnection, we use the Geocentric Solar Magnetospheric Coordinate System, called the GSM system, with x axis pointing toward the sun, y axis from dawn to dusk perpendicular to x axis and the Earth's magnetic dipole axis. In general, the planet's magnetic dipole axis has a tilt angle θ with respect to the mutually perpendicular z axis.

Here we investigate a relatively simple nonlinear electron scale magnetic reconnection model based on two nonlinear partial differential equations for the magnetic flux $\psi(x,z,t)$ and the electrostatic potential $\phi(x,z,t)$ that describe in the final state a release of magnetic energy $-\Delta E_B$ of order 50% available from the reversed field components $\pm B_{x0}$ in a volume of $\Omega=L_xL_yL_z\sim 2000d_e^2L_y$.

We show that during the reconfiguration period there is a interval of time, in the initial evolution of the magnetic island, during which the $\boldsymbol{E}\times\boldsymbol{B}$ flow energy dominates the parallel flow energy and the electron thermal energy. Subsequently the power transfer to the electron pressure $\delta P_e=\delta nT_e$ is dominant.

Indeed, in the early nonlinear phase, the magnetic island associated to the instability undergoes an explosive growth, which confirms the theoretical predictions of Ottaviani and Porcelli[4] and Bhattacharjee *et al.*[5] In this first phase, most of the power transfer goes to the $\boldsymbol{E}\times\boldsymbol{B}$ flow (around 70% of $|\Delta E_B|$).

However, when islands on neighboring resonant surfaces start to interact, the system becomes turbulent. The $\boldsymbol{E}\times\boldsymbol{B}$ energy decreases initially in favor of the parallel electron flows energy, $K_\parallel=1/2n_em_eu_\parallel^2$, and finally to the electron thermal energy, $\Delta W_e=3/2\Delta p_e\Omega$. As the energy unit scale in the theory, we use the initial reversed field energy per unit length along the ambient current: $E_{B0}=B_{x0}^2L_xL_z/(2\mu_0)$. In the given numerical example in Fig. 2(a), the energy release in the turbulent state, i.e., $-\Delta E_B$, is approximatively 70% of the initial reversed field energy E_{B0}. Of this released magnetic energy, approximately 44% goes to electron thermal energy, 47% to parallel electron flow kinetic energy, $K_\parallel$, and 9% to $\boldsymbol{E}\times\boldsymbol{B}$ flow kinetic energy. The key pathways for the power transfer are shown in Fig. 1.

In the model, there are four nonlinear terms and two key kinds of power transfer terms, $J_\parallel\nabla_\parallel\phi$ and $v_{e\parallel}\nabla_\parallel p_e$, as shown in Fig. 1. A third nonlinear transfer, the $\boldsymbol{E}\times\boldsymbol{B}$ convection of the plasma vorticity, $U=\nabla_\perp^2\phi/B_0$, derived from $\boldsymbol{v}_E=\boldsymbol{E}\times\boldsymbol{B}/B_0^2$ with $\boldsymbol{E}=-\boldsymbol{\nabla}\phi$ and $B_0\hat{\mathbf{y}}$ the out-of-plane guide field, arising from the ambient dawn-to-dusk magnetic field in the geomagnetic tail. The vorticity nonlinearity, $\boldsymbol{v}_E\cdot\boldsymbol{\nabla}U$, is well known and was recently measured by Perez *et al.*[6] in the LArge Plasma Device (LAPD). Its effect is to couple energy throughout the cross-field flow wavenumber spectrum, $|\phi_{\boldsymbol{k}}(t)|^2$, which appears in the configuration space as vortex merging. Thus, this vorticity nonlinearity has only an indirect effect in the dynamics of the reconnection, which accounts for its being dropped in the model of Ref. 4.

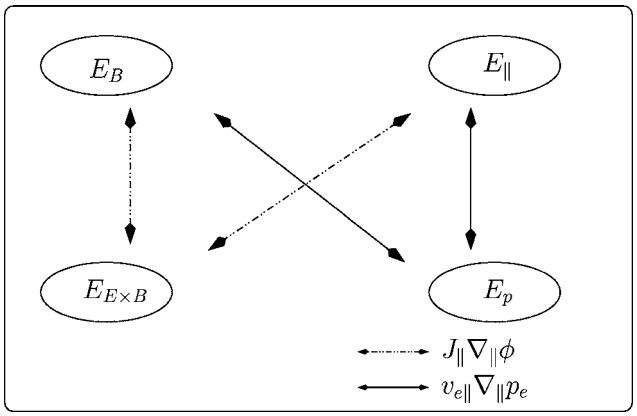

FIG. 1. Diagram of the energy transfer among magnetic energy E_B, perpendicular kinetic energy $E_{E\times B}$, parallel kinetic energy $E_\parallel$, and electron thermal energy E_p. The nonlinear transfer powers are from $J_\parallel \nabla \phi$ with $J_\parallel = -en_e u_{\parallel e}$ and $J_\parallel \nabla p_e$, where p_e is the electron thermal pressure.

II. ELECTRON-SCALE MAGNETIC RECONNECTION MODEL

The latest developments on the electron-scale magnetic reconnection modes are given in Ottaviani and Porcelli[4] and Bhattacharjee *et al.*[5] The impulsive reconnection model of Bhattacharjee has the field-line-breaking mechanism of electron inertial given by finite $d_e = c/\omega_{pe}$. Therefore, it is necessary to use the generalized Ohm's law

$$\boldsymbol{E} + \boldsymbol{v} \times \boldsymbol{B} = \frac{c^2 \mu_0}{\omega_{pe}^2} \frac{d\boldsymbol{J}}{dt} - \frac{\boldsymbol{\nabla} p_e}{ne} + \frac{\boldsymbol{J} \times \boldsymbol{B}}{ne} + \eta \boldsymbol{J}, \tag{1}$$

where $\boldsymbol{E}$ is the electric field, $\boldsymbol{B}$ is the magnetic field, $\boldsymbol{v}$ is the plasma flow velocity, c is the speed of light, $\boldsymbol{J}$ is the current density, p_e is the electron pressure, ω_{pe} is the electron plasma frequency, n is the electron density, and e is the magnitude of the electron charge.

In the simulations shown here, we take the limit of zero plasma resistivity η and check energy conservation to five digits. High-order time integrator techniques allow us to run simulations for finite times with zero resistivity.

The simplest electron tearing mode dynamics occurs when plasma flow is almost incompressible. This occurs when there is a guide field B_y. Although the guide field is not thought to be important to the real event, it is included in our treatment to make a simple justification of dropping the dynamics of the electron pressure equation.

The small flow compression comes from the polarization drift of the ions and is given by $\partial U/\partial t$, where $U = \nabla_\perp^2 \phi / B_y$, with $\boldsymbol{E} = -\partial \psi/\partial t \hat{\mathbf{y}} - \boldsymbol{\nabla} \phi$ and $\boldsymbol{B} = \boldsymbol{\nabla} \psi \times \hat{\mathbf{y}} + B_y \hat{\mathbf{y}}$. The vorticity U grows to feed plasma into the reconnection layer. The compressional Alfvén wave drops out of the dynamics in this regime owing to its higher frequency and different polarization.

The plasma is described in an electron-Hall fluid limit by the following two field equations:

$$\frac{\partial F}{\partial t} + [\phi, F] = \hat{\rho}_s^2 [U, \psi], \tag{2}$$

$$\frac{\partial U}{\partial t} + [\phi, U] = [J, \psi], \tag{3}$$

where $J = -\nabla_\perp^2 \psi$, $F = \psi + \hat{d}_e^2 J$, $U = \nabla_\perp^2 \phi$, and the Poisson bracket is defined by $[\phi, F] = \hat{\mathbf{y}} \cdot \boldsymbol{\nabla} \phi \times \boldsymbol{\nabla} F$. All quantities are dimensionless (this will be fixed with the proper dimensions). Time is normalized by Alfvén time scale $\tau_A = l_z/v_A$, where the Alfvén velocity $v_A = \sqrt{B^2/\mu_0 \rho}$ and $l_z = L_z/2\pi$ is the scale over which the ambient current density varies. The dynamics depends on two dimensionless parameters $\hat{d}_e$ and $\hat{\rho}_s$, where the electron skin depth $\hat{d}_e = (c/\omega_{pe})/l_z$ and the ion sound gyro radius $\hat{\rho}_s = (c_s/\omega_{ci})/l_z$.

In the region of a uniform $B_x = \partial \psi/\partial z$ field, the linearized dynamics from Eqs. (2) and (3) gives $\omega F_k - k_x B_x \phi_k = \rho_s^2 k_x B_x U_k$ and $\omega U_k = -k_x B_x J_k$. Therefore, we obtain

$$\omega^2 = \frac{k_x^2 v_A^2 (1 + k_\perp^2 \hat{\rho}_s^2)}{1 + k_\perp^2 \hat{d}_e^2} \tag{4}$$

which is the well-known kinetic Alfvén wave dispersion relation. The properties of these waves in a uniform plasma have recently been studied experimentally by Vincena *et al.*[7] in the LAPD. Here we follow the formulation of Bhattacharjee *et al.*[5] and Ottaviani and Porcelli,[4] but note there is an important error in the magnetic flux function equation in Bhattacharjee *et al.*[5] That error is corrected here in Eq. (2). The error in the $\rho_s^2 [U, \psi]$ term would completely eliminate the energy conservation derived here. The same model has been used in Cafaro *et al.*[8] and Grasso *et al.*,[9] where the formation of fine structures and the saturation of a single magnetic island are investigated. In particular, Grasso *et al.*[9] presented a numerical study of the energetics of an isolated island, by using an Harris pinch equilibrium.

Owing to the absence of boundaries in the central plasma sheet and the nonmonotonic nature of the cross-tail current density $J_y(z)$, periodic box boundary conditions, as those in Bhattacharjee *et al.*,[5] are more appropriate in our investigation.

The computation has been done with

$$\psi = \Sigma_{n,m} \psi_{m,n}(t) \exp(inz + im\epsilon x), \tag{5}$$

$$\phi = \Sigma_{n,m} \phi_{m,n}(t) \exp(inz + im\epsilon x), \tag{6}$$

where n, m are integers, and $\epsilon = L_z/L_x = l_z/l_z$ is an aspect ratio of the system. The initial profile are the unstable current sheet $\psi_{0,1}$ with small perturbations $\psi_{1,4}$ and $\phi_{1,4}$; that is,

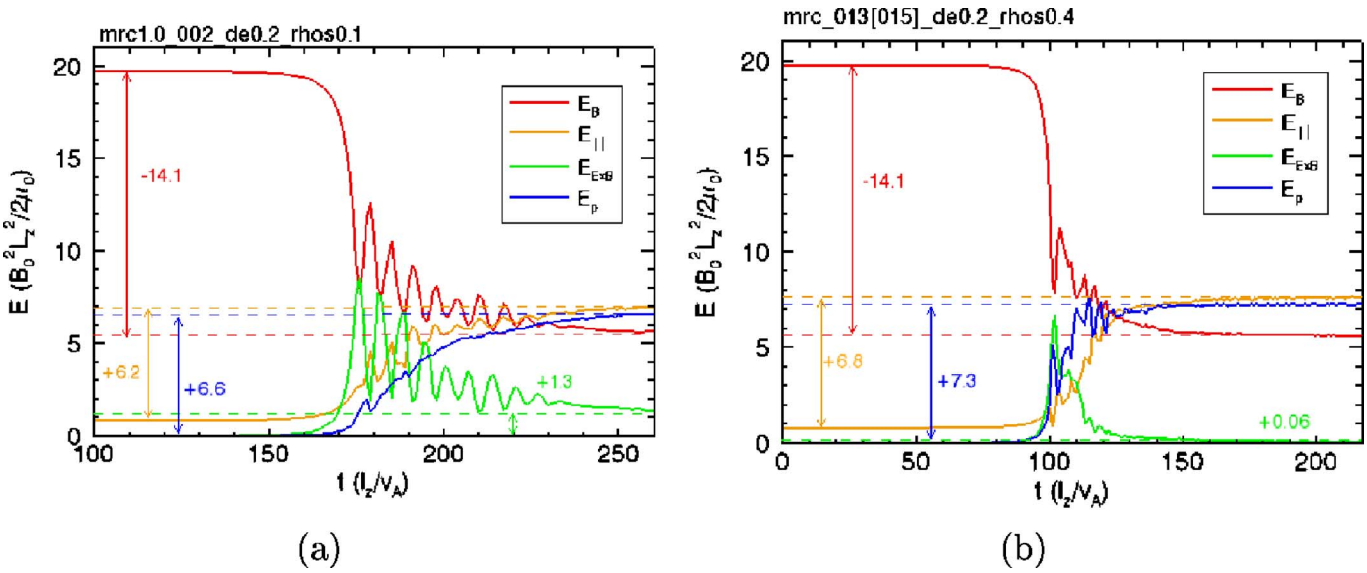

FIG. 2. Time evolution of magnetic energy E_B (red), parallel electron flow energy $E_\parallel$ (orange), perpendicular $\boldsymbol{E}\times\boldsymbol{B}$ energy (green), and electron thermal energy E_p for small and large ρ_s values. (a) $\hat{d}_e=0.2, \hat{\rho}_s=0.1$ and (b) $\hat{d}_e=0.2, \hat{\rho}_s=0.4$ with initial mode $(k_x,k_z)=2\pi(4/L_x, 1/L_z)=2\pi(0.5,4)/L_z$. Approximately 70% of initial magnetic energy is released in the cases (a) and (b)

$$\psi(0) = \cos z + \delta\psi \cos(4z)\cos(\epsilon x),$$

$$\phi(0) = \delta\phi \sin(4z)\sin(\epsilon x).$$

For the example shown here, with initial $\psi_{1,4}=\phi_{1,4}=0.0001$ there are 10 e-folding to reach the first maximum of $-E_B$ in Fig. 2. Other initial conditions $(n=2)$ with a spectrum of small modes leads to the same conclusions.

The simulation box is $L_z\times L_x=10\pi c/\omega_{pe}\times 20\pi c/\omega_{pe}$ and the unit of energy is $E_0=B_0^2L_z^2/2\mu_o$, which for a 10 nT reversed field over a $l_z=5c/\omega_{pe}=50$ km is 2.5×10^6 J/R_E.

Equations (2) and (3) are solved numerically in a double periodic box, with three resonant surfaces at $z=0$ and $z=\pm\pi$. The periodic boundary conditions used in our numerical analysis are justified by the fact that we are interested in the investigation of the dynamics of interacting microscale magnetic islands. The use of periodic boundary conditions is the standard model in condensed matter physics for eliminating the influence of surface effects in bulk matter calculations. Similarly, the physics of the boundary conditions at the lobe plasma and the magnetopause can be eliminated by assuming periodicity at the edge of the numerical box when its size is large compared with c/ω_{pe}, but small compared to the dimensions of the current sheet.

Note that the theoretical models of Ottaviani and Porcelli[4] and Bhattacharjee *et al.*[5] apply only to the early nonlinear phase of our numerical calculation, when the magnetic islands do not interact with each other. This is due to the fact that both models rely on the standard Rutherford nonlinear growth theory for single islands.[10] In particular, the existence of a dominant harmonic in the nonlinear magnetic flux is not a valid ansatz for the interacting islands arising in the late phase of our simulation. For this reason, the numerical integration in Bhattacharjee *et al.*[5] is stopped when the width of the central magnetic island becomes comparable to the system size. The simulations presented here are continued farther in time, roughly twice as long as those in Bhattacharjee *et al.*[5]

The electron reconnection model conserves the total energy of electrons and the magnetic field. The energy component formulas and the conservation law are given by

$$\frac{dE_{\rm tot}}{dt} = \frac{d}{dt}(E_B + E_\parallel + E_{E\times B} + E_p)$$
$$= \frac{1}{2}\frac{d}{dt}\int dxdz\{(\nabla\psi)^2 + d_e^2(\nabla^2\psi)^2 + (\nabla\phi)^2$$
$$+ [\rho_s^2(\nabla^2\phi)]^2\} = 0, \quad (7)$$

where E_B is magnetic energy, $E_\parallel$ is electron parallel flow energy, $E_{E\times B}$ is the electron perpendicular flow energy, and E_p is the electron thermal energy. As shown in Fig. 1, there are four transfers between the different energy components. The magnetic energy E_B and the electron parallel flow energy $E_\parallel$ are transferred back and forth to the thermal energy E_p by thermal interaction $\langle v_{e\parallel}\nabla_\parallel p_e\rangle$. In addition, the energies, E_B and $E_\parallel$, are transferred back and forth to the perpendicular flow energy $E_{E\times B}$ by the electric interaction $\langle j_\parallel\nabla_\parallel\phi\rangle$.

The time history of the energy relevant to the ϕ, U, ψ and J fields are shown in Fig. 2. During the saturation process, almost 70% of the magnetic energy is released and about 45%–50% of the released energy is transferred to the electron thermal energy. In Fig. 2(a), we see the released magnetic energy ΔE_B of 14.1 E_0 and the increase of the parallel flow kinetic energy in the electrons is 6.2 E_0. In the bottom panel, the perpendicular flow energy increases first to 8 E_0 and then drops to 1.3 E_0, while the electron thermal energy continually increases to 6.6 E_0. Energy is conserved by the 14.1 units of released magnetic energy going to 6.2 +6.6+1.3 (E_0 unit) units of parallel flow, perpendicular flow,

and thermal plasma energies, respectively. In terms of fractional changes, this is approximately a 70% decrease of magnetic energy transformed into 9% $E\times B$ flow, 44% parallel flow, and 47% electron thermal energy. The space and time scales are $10c/\omega_{pe}$ and $60L_z/v_A$, respectively. In the central plasma sheet, these scales are typically 100 km and 1 min.

In Fig. 2(b), the case of $\hat{d}_e=0.2$, $\hat{\rho}_s=0.4$ shows the energy release 70% of the magnetic energy and the transfer of 40%, 0.4%, and 52% to the parallel flow energy, the $\boldsymbol{E}\times\boldsymbol{B}$ energy, and the thermal energy, respectively. The twice larger $\hat{\rho}_s$ corresponds to a four times large $\nabla_\parallel p_e$ term in Ohm's law, which makes the transition faster, as shown in Fig. 1, and increases the final electron thermal energy from 6.6 to 7.3 E_0.

When Eqs. (2) and (3) are run as written with no dissipation, the magnetic energy drops sharply over a period of 10 to 50 Alfvén time and the high-k spectrum increases until subscale energy dissipation is required or the simulation is stopped in time. For a convergence test, the simulations are then repeated with hyper-resistivity $\eta_4(\nabla^2)^4F$ and hyperviscosity $\mu_4(\nabla^2)^4U$ added to the right-hand side. Now, wavenumber spectra are compared. We find that the wavenumber spectra in the range $k_\perp=[1,20]/L_z$ are essentially the same. For $k_\perp$ greater than or equal to $30/L_z$, there is a rollover and a rapid drop-off for the runs with high-k damping.

We have investigated the background electron temperature gradient effect with two parallel heat closure models. The first one is an electrostatic closure model. The parallel heat flux convected by $\boldsymbol{E}\times\boldsymbol{B}$ velocity without the consideration of the magnetic fluctuation is zero. This model needs a large but finite parallel heat diffusivity $\chi_{e\|}$. Thermal balance reduces to

$$n\boldsymbol{v}\cdot\boldsymbol{\nabla}T_e+\nabla_\parallel q_{e\|}=0 \tag{8}$$

with $q_{e\|}=-n\chi_{e\|}\nabla_\parallel T_e$, where Sugama *et al.*[11] give a model for $\chi_{e\|}$. The electron temperature fluctuation is

$$\frac{\delta T_e}{T_e}=-i\frac{\omega_{*Te}}{\chi_{e\|}k_y^2}\frac{e\phi}{T_e}, \tag{9}$$

where $\omega_{*Te}=k_xT_e/eB_yL_{Te}$. The second model is an electromagnetic closure model. The parallel thermal diffusivity is taken as infinitely large and the parallel heat flux $q_{e\|}$ is bounded from above. This means the magnetic fluctuation is governed by

$$\nabla_\parallel T_e=\frac{\partial\delta T_e}{\partial y}+\frac{\delta\boldsymbol{B}}{B_y}\cdot\boldsymbol{\nabla}T_e=0, \tag{10}$$

reducing to

$$\frac{\delta T_e}{T_e}=\frac{\omega_{*Te}}{ck_y}\frac{ce\psi}{T_e}. \tag{11}$$

The presence of finite $\delta T_e/T_e$ adds to the right-hand side of Eq. (2) as $[U,\psi]\rightarrow[U+\delta T_e/T_e,\psi]$. The simulations have been performed with this modification of the system. At the small values of $\omega_{*Te}/\chi_{e\|}k_y^2$ and ω_{*Te}/ck_y, we did not observe a significant effect, and we need to investigate further. Drake and Lee[3] reported that the electron temperature gradient does not cause the instability in collisionless regime.

III. CONCLUSION

We have shown that the electron reconnection scale produces fast, small scale releases of stored, reversed field magnetic energy. In laboratory experiments, the calculations are typically performed for a few, well separated magnetic islands, as observed from soft x-ray emissions in tokamaks. However, in the present work we do not stop the simulations in order to consider only the isolated island evolution, but continue them into the interesting regime of strong island interactions. The pseudospectral simulations with high order time integration can resolve the strong nonlinear state down to the scale where microturbulence from lower hybrid drift waves would be expected. We note that the current densities reported in the Cluster spacecraft geotail data have peak values with drift velocities of order twice the ion thermal velocity.

The dynamics exhibits a long exponential growth, ending with a nonlinear pulse that is faster than linear growth. Finally, saturation is reached in a turbulent state. Typically, 70% of the initial magnetic energy, which is the difference of the magnetic energy in two different magnetic field geometry, is redistributed into the sum of the parallel and perpendicular flow energies and the electron thermal pressure by the reconnection pulse.

The model developed here is missing the kinetic physics of the wave-particle interactions. Thus, the simulation alone is not able to capture the beam-like features of the ion and electron velocity distribution, reported by spacecraft particle detectors. Some of these features maybe captured by adding ensembles of test particles to be integrated with the evolving reconnection electromagnetic fields. An example of this technique can be found in Horton and Tajima,[12] where the strong ion energization is shown for a simple analytic model of the ion-tearing mode.

The physical nature of the ion tearing mode is far from clear. We note that a common formulation of Ohm's law (ion Hall magnetohydrodynamics) for the ion tearing mode is

$$\boldsymbol{E}=-\boldsymbol{v}\times\boldsymbol{B}+\frac{\boldsymbol{J}\times\boldsymbol{B}}{ne},$$

which keeps $E_\parallel=\boldsymbol{E}\cdot\boldsymbol{b}=0$ so that the magnetic flux is not reconnected (Biskamp,[13] p. 16). In the case in which the $\boldsymbol{B}\cdot\boldsymbol{\nabla}\cdot\boldsymbol{P}_i$ is large, magnetic reconnection does occur. An example of this type of ion reconnection is analyzed in Horton and Tajima.[12] This is a type of chaotic ion viscous dissipation that frees the magnetic field from the assumption of the frozen-in theorem.

Some kinetic theory physics, such as that related to a finite ion gyroradius, can be added to the partial differential equations. Perhaps the most important kinetic effect to be added to the fluid model is the electron temperature fluctuation, δT_e. This is driven by the $\tilde{\boldsymbol{v}}_E\cdot\boldsymbol{\nabla}T_e$ convection in the nonuniform background T_e field. This addition has been briefly investigated. The background temperature gradient introduces the drift-tearing mode physics, thought to be an important instability for electron thermal transport in high-β laboratory confinement experiments. The simplest version of this modification is to generalize the right-hand side of Eq.

(2) to $\hat{\rho}_s^2[U+\eta_e\partial_x\phi,\psi]$, where η_e measures the nonuniformity of the ambient electron temperature profile.

The electron reconnection event similar to that modelled here may have been observed with a substorm of August 24, 2003 during a period when the Cluster space crafts crossed a thin current sheet $L_j \leqslant 2c/\omega_{pi} \approx 1000$ km and measured electron acceleration and tailward high speed flows. The event was found in the Cluster 2003 tail season data by Nakamura *et al.*.[14] The current sheet is comparable to the ion collisionless skin depth in thickness as the four spacecraft with a spacing of 200 km flew through the geotail. The event was found by selecting data with high current densities. The current density for this event reached 40 $\mathrm{nA/m^2}$, which is about ten times the nominal value for the center of the current sheet. The spacecraft were at approximately $(-17, -3.8, 3.3)$ R_E in the geotail. The electron energy flux and pitch angle distribution are observed to increase from 0.5–0.8 keV up to 5 keV in crossing a turbulent reconnection zone. Electron acceleration reported during this reconnection event is suggestive of the electron reconnection dynamics analyzed in this present work.

A second example[15] of a microscale magnetic reconnection event is described by 15-min Cluster repeated crossings of a moving plasma sheet at distance $x=-16$ R_E in the midnight sector. This event was measured during the geomagnetic storm of October 1, 2001. The electric and magnetic fields are measured every 50 ms and the particle distribution every 8 s. In the 15-min interval, the signature of the c/ω_{pe}-scale reconnection dynamics are seen. The density is 0.1 $\mathrm{cm^{-3}}$, giving $c/\omega_{pe}=20$ km. The measured magnetic field reverses from $B_x=\pm 15$ nT over a current sheet of thickness $\sim 5c/\omega_{pe}$ in 4 s, from the motion of the spacecraft through the current sheet. The guide field, B_y, is approximately 5 nT. The plasma parameters upstream $(\beta \ll 1)$, in the layer $(\beta \geqslant 100)$, and downstream appear to be consistent with the magnetic reconnection model described in this work.

ACKNOWLEDGMENTS

This work is supported by the NSF Grant ATM-0539099 and by a Center for Multiscale Plasma Dynamics Grant DoE DE-FC 02-04ER54784.

[1] B. Coppi, G. Laval, and R. Pellat, Phys. Rev. Lett. **16**, 1207 (1966).
[2] B. Kadomtsev, Sov. J. Plasma Phys. **1**, 389 (1975).
[3] J. F. Drake and Y. C. Lee, Phys. Fluids **20**, 1341 (1977).
[4] M. Ottaviani and F. Porcelli, Phys. Rev. Lett. **71**, 3802 (1993).
[5] A. Bhattacharjee, K. Germaschewski, and C. S. Ng, Phys. Plasmas **12**, 042305 (2005).
[6] J. Perez, W. Horton, K. Gentle, W. Rowan, K. Lee, and R. Dahlburg, Phys. Plasmas **13**, 032101 (2006).
[7] S. Vincena, W. Gekelman, and J. Maggs, Phys. Rev. Lett. **93**, 105003 (2004).
[8] E. Cafaro, D. Grasso, F. Pegoraro, F. Porcelli, and A. Saluzzi, Phys. Rev. Lett. **80**, 4430 (1998).
[9] D. Grasso, F. Califano, F. Pegoraro, and F. Porcelli, Phys. Rev. Lett. **86**, 5051 (2001).
[10] P. H. Rutherford, Phys. Fluids **16**, 1903 (1973).
[11] H. Sugama, T. H. Watanabe, and W. Horton, Phys. Plasmas **8**, 2617 (2001).
[12] W. Horton and T. Tajima, J. Geophys. Res. **96**, 15811 (1991).
[13] D. Biskamp, *Magnetic Reconnection in Plasmas* (Cambridge Univerity Press, Cambridge, 2000).
[14] R. Nakamura, W. Baumjohann, Y. Asano, A. Runov, A. Balogh, C. J. Owen, A. N. Fazakerley, M. Fujimoto, B. Klecker, and H. Reme, J. Geophys. Res. **111**, A11206 (2006).
[15] J. R. Wygant, C. A. Cattell, R. Lysak *et al.*, J. Geophys. Res. **110**, A09206 (2005).